processes

MDPI

Article

Adsorbent Biomaterials Based on Natural Clays and Orange Peel Waste for the Removal of Anionic Dyes from Water

Sonia Mihai, Andreea Bondarev *, Cătalina Călin and Elena-Emilia Sîrbu

Chemistry Department, Petroleum-Gas University of Ploiesti, 39 Bucharest Blvd., 100680 Ploiesti, Romania; smihai@upg-ploiesti.ro (S.M.); catalina.calin20@yahoo.com (C.C.); oprescuemilia@gmail.com (E.-E.S.)
* Correspondence: andreeabondarev22@gmail.com

Abstract: This study demonstrates the efficient removal of Alizarin Yellow R anionic dye (AY) from aqueous solutions using green adsorbents. Natural kaolin clay (A1), acid-modified natural clay (A2), chemically treated orange peel (C1) and biochar produced by the thermal treatment of orange peel (C2) were tested for the adsorption of AY. The characteristics of the sorbents were determined by instrumental methods: SEM, EDS, FTIR, BET and TGA. The adsorption experiments were performed under different conditions, including the initial AY dye concentration, adsorbent weight, *p*H, temperature and contact time. The maximum adsorption capacities had values between 15.72 and 74.62 mg/g at 298 K and the optimal *p*H of 6.5 at initial concentrations ranging from 30 to 70 mg/L for all adsorbents. The equilibrium data were used for the adsorption isotherm models: Freundlich, Langmuir and Temkin. The Freundlich model fit best for the adsorbents A2, C1 and C2, and the Langmuir isotherm had the highest regression value for the adsorbent A1 (R^2 = 0.9935). Thermodynamic parameters indicated the spontaneous and favorable adsorption process of AY. A study of the adsorption kinetics proved that they best fit the pseudo-second-order model, with the highest coefficients of determination (R^2), outperforming the pseudo-first-order model. The results of this study indicate the potential for the valorization of locally available clays and orange peel waste in the purification processes of water.

Keywords: dye removal; adsorption; natural clay; orange peel; equilibrium isotherm; thermodynamics; adsorption kinetics

Citation: Mihai, S.; Bondarev, A.; Călin, C.; Sîrbu, E.-E. Adsorbent Biomaterials Based on Natural Clays and Orange Peel Waste for the Removal of Anionic Dyes from Water. *Processes* **2024**, *12*, 1032. https://doi.org/10.3390/pr12051032

Academic Editor: Antoni Sanchez

Received: 11 April 2024
Revised: 16 May 2024
Accepted: 17 May 2024
Published: 19 May 2024

1. Introduction

Synthetic dyes are widely used in many industrial sectors, especially in the textile industry. Most dyes are generally dangerous and toxic to the environment and organisms. Various azo dyes have carcinogenic effects and can have serious health consequences, such as dermatitis, inflammation of the mucous membranes, irritation of the respiratory tract and allergic eye reactions [1–3].

Dyes are typical organic pollutants derived from industrial waste from the textile, leather, paper, plastics, cosmetic and food industries. All types of Alizarin dyes (Alizarin Yellow R, Alizarin Yellow GG, Alizarin Red C) are commonly used as indicators and as dyes in the textile industry. The release of chemically modified forms of Alizarin dyes into the environment does not result in their biodegradation and can cause considerable damage [4].

Various conventional techniques, such as precipitation, chemical degradation, chemical coagulation, adsorption and biodegradation, have been explored to remove dyes from water. The environmental pollution caused by these compounds is significant, and they can generate hazardous by-products in the receiving medium through oxidation or other chemical processes [3,5].

Conventional methods of wastewater treatment have some difficulties in removing dyes from wastewater because these compounds are not biodegradable and persist under light sources and with exposure to oxidizing chemicals [6–8].

The adsorption process is regarded as an effective method for removing water contaminants because it has the following advantages over other methods: cleanliness, ease of application and low cost. To reduce the cost of treatment to remove various dyes, numerous research studies in recent years have focused on the search for low-cost, biodegradable and highly effective adsorbents that are available locally. In general, an adsorbent can be considered low-cost if it can be produced from natural resources or agricultural waste, needs little processing and is waste or a by-product from different industrial sectors [3,6,9–11].

Due to the different physico-chemical properties of various sorbents, the adsorption capacity also varies. The selection of an adsorbent affects the efficiency of removing toxic compounds from the aqueous environment. Therefore, an important research topic is the synthesis and processing of cost-effective and highly efficient adsorbents for various pollutants [3,12].

Nanomaterials include materials with a size of less than 100 nm, and they have been tested as adsorbents of wastewater pollutants such as inorganic and organic compounds. Various nanocomposites, iron oxide nanoparticles and clay nanoparticles are considered effective adsorbents for the removal of pollutants from aqueous solutions [13].

Environmentally friendly and inexpensive materials that are abundant in nature, such as natural clays, have been cited by numerous researchers as potential adsorbents for inorganic and organic pollutants [2,3]. The specific properties of natural clays, such as their large surface area and specific cation-exchange capacity, suggest their good potential for the removal of numerous organic and inorganic pollutants. A number of activation methods have been reported, and the most common techniques include mechanical activation and thermal activation. Despite their advantages, these activation methods have some limitations, for example, their application to multimineral and mixed-layer clays [2,3]. A common activation method for natural clays is chemical modification, usually of bentonites, with a solution of a mineral acid or a base. These methods are used to obtain materials with increased specific surface area and to increase their porosity and surface acidity. Acid-activated clays are of significant interest as adsorbents and catalysts for a range of research studies. In this context, the application of natural clays as efficient adsorbent materials has received attention in many research studies due to their low cost and wide availability [2,3,13–16].

Carbonaceous biomass derived from plants is found in the form of agricultural waste. They are produced from renewable sources that are non-toxic, active in recycling and cost-effective. Numerous research studies have shown that agricultural waste has great potential for use as an adsorbent due to its specific properties and vast biomass resources [17]. Carbonization is an efficient method for using biomass resources and treating pollutants in water while solving energy shortage and ecological imbalance problems [17,18]. Various studies in the literature on the adsorption of different pollutants using orange peels have identified the properties of this natural material that could impact the adsorption process of pollutants and assessed the adsorption performance in different experimental conditions [15,17]. The chemical composition of orange peel consists mainly of organic substances. Several studies on the physical properties of orange peels have shown that they contain soluble sugars, starch and fiber, including cellulose, hemicellulose, pectin and lignin, protein and about 1% organic acids [11]. Orange peels are agro-industrial waste from beverage industries around the world and are used to remove inorganic pollutants, colorants and some organic compounds [11,12,18].

Biochar, a carbon-rich solid extracted from biomass in low-oxygen conditions, is now widely used as an absorbent due to its low cost, large surface area and rich pore structure. The various sources from which biochar is derived include plant roots, fruit and vegetable waste, organic waste, wheat straw, sewage sludge and other biomass resources [12,18].

The current study evaluates the potential of two biomaterials—natural clay and orange peel waste—to obtain bio-adsorbents for the removal of Alizarin Yellow R dye (AY) from aqueous solutions. The available scientific literature lacks documented research into the effectiveness of these adsorbent materials in removing Alizarin Yellow R from aqueous

solutions. The current study represents an opportunity to explore a new approach and evaluate its potential as an effective method for the removal of this anionic dye.

The adsorbents used in our studies were natural kaolin clay (A1), acid-modified natural clay (A2), chemically treated orange peel (C1) and thermally treated orange peel (C2). The influence of different experimental factors, such as adsorbent weight, the initial concentration of AY dye, *p*H, adsorbent–dye contact time and temperature, were analyzed to evaluate the possibility of using the tested adsorbents for Alizarin Yellow R dye removal.

To examine the potential interactions between AY molecules and adsorbents, three mathematical models, Langmuir, Freundlich and Temkin, were used to compare the adsorption equilibrium results and to evaluate them. Thermodynamic parameters were determined, and the adsorption behavior of AY was also investigated in kinetic studies.

2. Materials and Methods

2.1. Preparation of Model Water

All chemicals used in this study were of analytical grade.

Alizarin Yellow R: 5-(3-Nitrophenylazo) salicylic acid sodium salt (analytical reagent, Sigma-Aldrich, Munich, Germany) was used to prepare a stock solution at a concentration of 500 mg/L. The AY stock solution was further diluted in demineralized water to obtain the necessary standard solutions (20–100 mg/L).

A calibration curve of AY dye was obtained by measuring the absorbance of known concentrations at the wavelength λ_{max} = 380 nm using a UV–Visible spectrophotometer (CECIL 1021, 1000 Series, Cambridge, United Kingdom). The residual concentration of AY was analyzed by UV-Vis spectroscopy, and the previously known calibration curve was used to determine the unknown dye concentration in each sample after adsorption.

The acidic or basic solution *p*H was adjusted by adding either 0.1 N HCl or 0.1 N NaOH. A digital multi-parameter (Multi 9630 IDS meter) equipped with a glass membrane-selective electrode (Xylem Analytics, Weilheim, Germany) was used to perform *p*H measurements.

2.2. Preparation of Adsorbents

2.2.1. Natural Clay Adsorbent

Natural clay, sourced from the Dobrogea region, Romania, was washed thoroughly with distilled water, without any chemical treatment. These clay samples were dried in an oven at 105 °C for 24 h, and they were milled and sieved to obtain a fine powder of nanoclay $\leq$ 125 μm.

After crushing, the sample powder was washed again with distilled water, and then the samples were oven-dried in the same conditions.

The natural clay adsorbent is henceforth referred to as A1.

2.2.2. Chemical Activation of Natural Clay

The acid activation of natural clay was performed with a sulfuric acid solution (0.1 N H_2SO_4). The modification in acid form increases the total pore volume and the specific surface of natural clays.

Each 5 g natural clay sample was added to a conical flask, treated with a 100 mL solution of 0.1 N H_2SO_4 and stirred continuously for 2 h; then, it was decanted and washed 3–4 times with distilled water until it was acid-free. The resulting solid was oven-dried at 105 °C for 24 h, and then it was milled and sieved to fine particles $\leq$125 μm. After crushing, the sample powder was washed again with distilled water, and then the samples were dried in the oven in the same conditions. The samples were stored in a desiccator.

Chemically treated natural clay is henceforth referred to as A2.

2.2.3. Chemical Modification of Orange Peel

The chemical modification of biomass can be directed to improve structural properties. Many research studies describe the effects of various chemicals on the structural properties of orange peels and the capacity of adsorption. The reported literature presents good adsorption

results after the treatment of orange peels with a base, which increased the binding sites of this sorbent [19,20]. The major components of orange peel are methyl esters, which can be transformed into carboxylates by treatment in a basic solution medium [21–23].

In this study, the orange peel waste was washed 2–3 times with demineralized water, and then it was cut into smaller portions and oven-dried at 105 °C for 24 h. The obtained dried orange peel was finely crushed and sieved to a powder with particle sizes ≤200 µm. The chemical treatment and modification of orange peel waste was carried out by adding a mixture of 0.5 M $CaCl_2$ and 0.5 M NaOH solutions to the solid material, followed by stirring for 4 h at 25 °C. This mixture was filtered, and the precipitate was washed with demineralized water until the neutral *p*H of the filtrate was obtained. The obtained material was dried for 8 h in an oven at 105 °C.

Chemically treated orange peel is henceforth referred to as C1.

2.2.4. Preparation of Biochar from Orange Peel

Biochar was prepared using a modified reported procedure [24]. Several recent research studies have presented the advantages of the process of biomass thermal treatment, which improves both the surface structure and the adsorption properties. The high-temperature calcination of orange peel waste was performed to obtain an enhanced adsorption capacity that could be explained by appropriate access to active adsorption sites [20,25–27]. In our study, dried orange peel raw material was first prepared in a few steps, as presented for the adsorbent C1, and thereafter, sieved fine particles with sizes ≤ 200 µm were carbonized at 500 °C in a muffle furnace (Nabertherm, Lilienthal, Germany). The samples of biochar prepared from orange peel waste were cleansed until the neutral *p*H of the filtrate was obtained, and then they were oven-dried at 105 °C for 24 h.

Activated carbon prepared by this method from orange peel is henceforth referred to as C2.

2.3. Characterization of Adsorbents

The surface morphology of the samples was studied by scanning electron microscopy (SEM) and energy-dispersive X-ray spectroscopy (EDS). SEM micrographs and EDS mapping images were obtained on a FIB-SEM at 30 kV (Thermo-Fisher, Brno, Czech Republic).

Fourier transform infrared spectra were collected in the range of 4000–400 cm^{-1} with a resolution setting of 4 cm^{-1} using a Shimadzu IR TRACER 100 spectrometer (Shimadzu, Kyoto, Japan).

Thermogravimetric analysis of adsorbents was performed using thermogravimetric/derivative equipment (TGA/DTG) (TGA 2 Star System Mettler Toledo, Zurich, Switzerland).

Texture parameters were determined at 77 K by a low-temperature nitrogen adsorption method using a Quantachrome NOVA 2200e system (Gratz, Austria). The specific surface area of the samples was calculated using a BET equation (Brunauer–Emmett–Teller).

2.4. Adsorption Equilibrium Studies

To evaluate the AY removal efficiency of the adsorbents, batch adsorption experiments were performed in different experimental conditions by continuous stirring using a rotary shaker (Benchtop 300X400MM, MUNRO, Essex, United Kingdom).

The adsorption of AY from synthetic solutions was studied in various conditions: the initial AY concentration (20–120 mg L^{-1}), adsorbent weight (0.2–1.2 g), temperature (25–40 °C), *p*H (2–10) and contact time (30–240 min). A volume of 100 mL of the AY solution was used.

The *p*H of the initial synthetic solutions was adjusted to the desired value using a 0.1 N HCl or 0.1 N NaOH solution and a *p*H electrode.

The adsorbent–AY samples were filtered and analyzed to determine the final concentration of AY dye and to characterize the adsorbents after adsorption.

The equilibrium adsorption capacity of the adsorbents (q_e, mg g^{-1}) was calculated using the following equation [1–6]:

$$q_e = (C_0 - C_e)\frac{V}{W} \quad (1)$$

The removal efficiency of AY dye (R%) was determined by the following equation [1–6]:

$$\% R = \frac{C_0 - C_e}{C_0} \times 100 \quad (2)$$

where C_0 represents the initial concentration of AY (mg L^{-1}), C_e is the equilibrium concentration of AY (mg L^{-1}), V corresponds to the solution volume (L), and W represents the mass of the sorbent (g).

3. Results and Discussion

3.1. Characterization of Adsorbents

3.1.1. Scanning Electron Microscopy Analysis

The surface morphology of the adsorbents was examined by scanning electron microscopy. Chemical composition analysis and elemental mapping were carried out using energy-dispersive spectroscopy (EDS). SEM images of adsorbents prepared from natural clay minerals (A1 and A2 samples) are exhibited in Figure 1a,b. High magnification reveals sheets with thicknesses of approximately 60 nm and lengths of several hundred nanometers, which are coated with fine nanosheets that tend to become agglomerated. The surfaces of these adsorbents present protuberances that are attributed to clay tactoids. Clay minerals are covered on their surfaces with layered silicates composed of Si and O bonds with other chemical elements, as observed in EDS spectra. These could be considered a stack of 2D single, double and multiple layers formed by SiO_4 tetrahedrons [28,29].

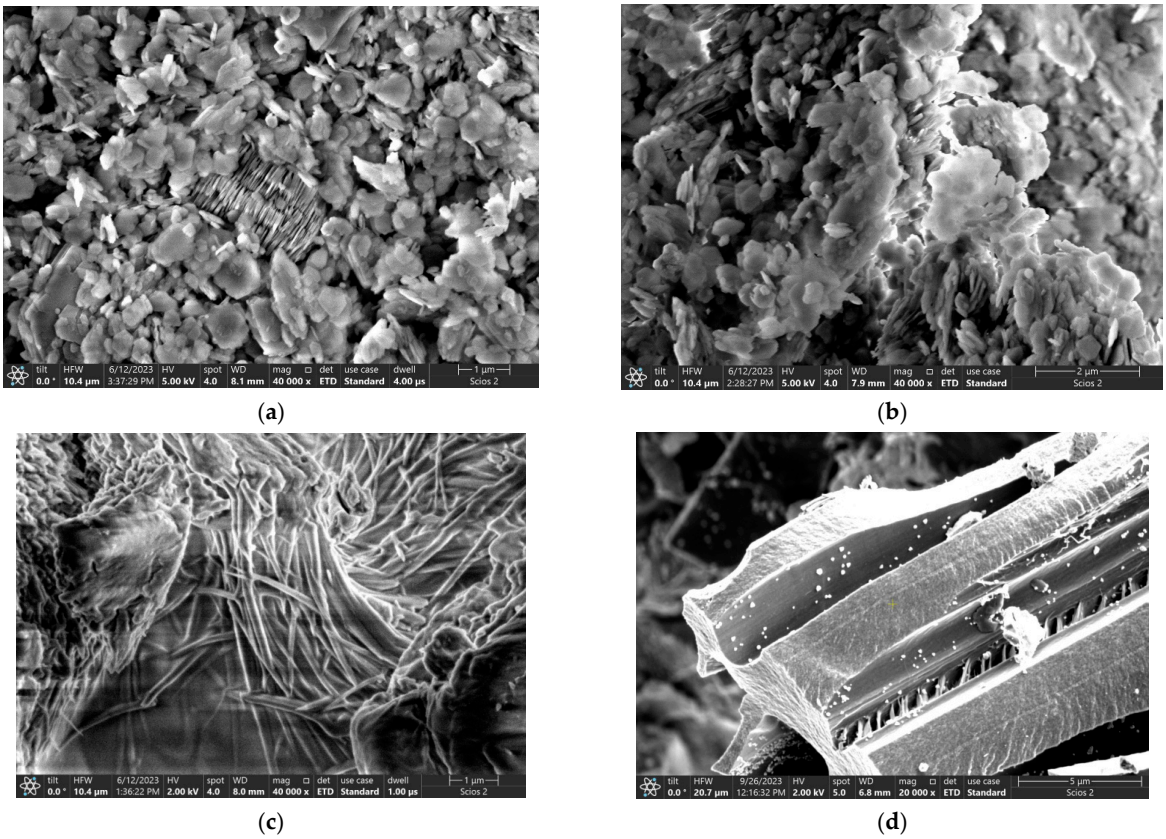

Figure 1. SEM images of the adsorbent samples: (**a**) A1; (**b**) A2; (**c**) C1; (**d**) C2.

The effect of acid activation can be observed for chemically treated natural clay. The sample of chemically treated natural clay in acid form (A2 adsorbent) has a porous, rough, irregular and heterogeneous structure, which are suitable properties of a good adsorbent.

EDS analyses (Figure S1—Supplementary Materials) performed randomly on different areas of the clay samples revealed the elements Si, Al, O and low concentrations of Cu for the natural clay (A1) sample and for chemically treated natural clay in acid form (A2 adsorbent sample).

Figure 1c illustrates the morphology of the chemically treated orange peel adsorbent C1, where the dehydrated organic structure of the orange peels can be observed. Intracellular spaces, cellulose, hemicelluloses and lignin fibers are also visible in the structure [30,31]. The biochar adsorbent prepared from orange peel waste—C2 (Figure 1d)—shows the characteristics of its precursor; complex three-dimensional structures with channels (cellulose matrix) and fibers (lignin matrix) originating from the elimination of organic matter can be observed. Figure 1d shows that the biochar prepared from orange peel waste contains thin pores, which could provide storage space for AY dye molecules.

EDS analyses (Figure S1—Supplementary Materials) performed randomly on different areas of the adsorbent samples prepared from orange peel waste evidenced C and O atoms and low concentrations of Si and Ca for the C1 adsorbent and the presence of C, O and lower concentrations of Zn, Al and Cu for the C2 biochar sample. The detection of the highest content of C atoms in the elemental composition of the biochar C2 sample proves the high purity of the adsorbent due to the thermal treatment. The low contents of Zn and Cu in this adsorbent could be attributed to Zn and Cu fertilizers combined with other agronomic management practices that are used in agriculture to sustain crop yields of Citrus trees.

3.1.2. ATR-FTIR Analysis

Functional groups present in the adsorbent materials were evidenced using ATR-FTIR spectroscopy. The FTIR spectra of clay adsorbent samples (A1, A2) and orange peel waste adsorbents (C1, C2) before the adsorption experiments and after AY dye sorption were examined in order to indicate the presence of functional groups that may play an important role in adsorption on the surface of sorbent materials (Figure 2). The FTIR spectrum of natural clay—the A1 sample (Figure 2a)—shows the characteristic absorption bands at 3694 and 917 cm^{-1} due to Al–Al–O stretching and bending vibrations. These absorption bands are more intense in the FTIR spectrum of chemically treated natural clay—the A2 sample (Figure 2) [29].

Orange peel contains –OH and –COOH functional groups, which represents an advantage in obtaining the good adsorption of polar organic compounds due to a chemical process. The chemical composition of orange peel can present some differences based on the region, growing conditions, variety and level of maturity. Orange peel mainly consists of organic matter; it contains starch, soluble sugar, fiber (cellulose, hemicellulose, lignin, pectin), proteins, ash, fats and a low content of organic acids [18].

The FTIR analysis of chemically treated orange peel (C1 sample) identified the most important functional groups that explain the adsorption process on the adsorbent surface. As we present in Figure 2, a broad absorption band observed at 3450 cm^{-1} corresponds to O–H bond stretching vibrations, which can be explained by inter-molecular hydrogen bonding. Weaker peaks at 2917 and 2850 cm^{-1} are assigned to the stretching vibrations of C–H bonds, and the absorption band at 1710 cm^{-1} proves the presence of carbonyl group stretching of ester bonds. A weak absorption band observed at 1410 cm^{-1} is assigned to C–H bond bending vibrations.

The absorption peak observed at 1050 cm^{-1} corresponds to the C–O stretching vibration mode (symmetric and asymmetric). This specific peak also indicates some functional groups of carbohydrates (C–OH and C–OR groups) [18,30,31].

The FTIR spectrum of the biochar adsorbent prepared from orange peel waste—the C2 sample—is displayed in Figure 2d; the most important absorption bands of the orange-

peel-based adsorbent C2 are –CH, $–CH_2$, –OH, –C–O and C=C. An intense absorption band observed at 3300 cm^{-1} is attributable to –O–H stretching vibrations, and the peak at 2869 cm^{-1} is assigned to–CH_2 stretching vibrations. The absorption bands at 1570 cm^{-1} and 1387 cm^{-1} are assigned to C=C stretching. A weak-intensity peak observed at the wavenumber 1022 cm^{-1} can be assigned to C–O bond stretching vibrations. Analyzing the characteristics of the orange-peel-based adsorbent C2 after thermal treatment, it could be observed that the majority of the characteristic functional groups' absorption peaks were eliminated. This modification can be explained by the fact that the functional groups of the adsorbent material were evaporated as volatile compounds during heating, also indicating a complete thermal activation process [26,32,33].

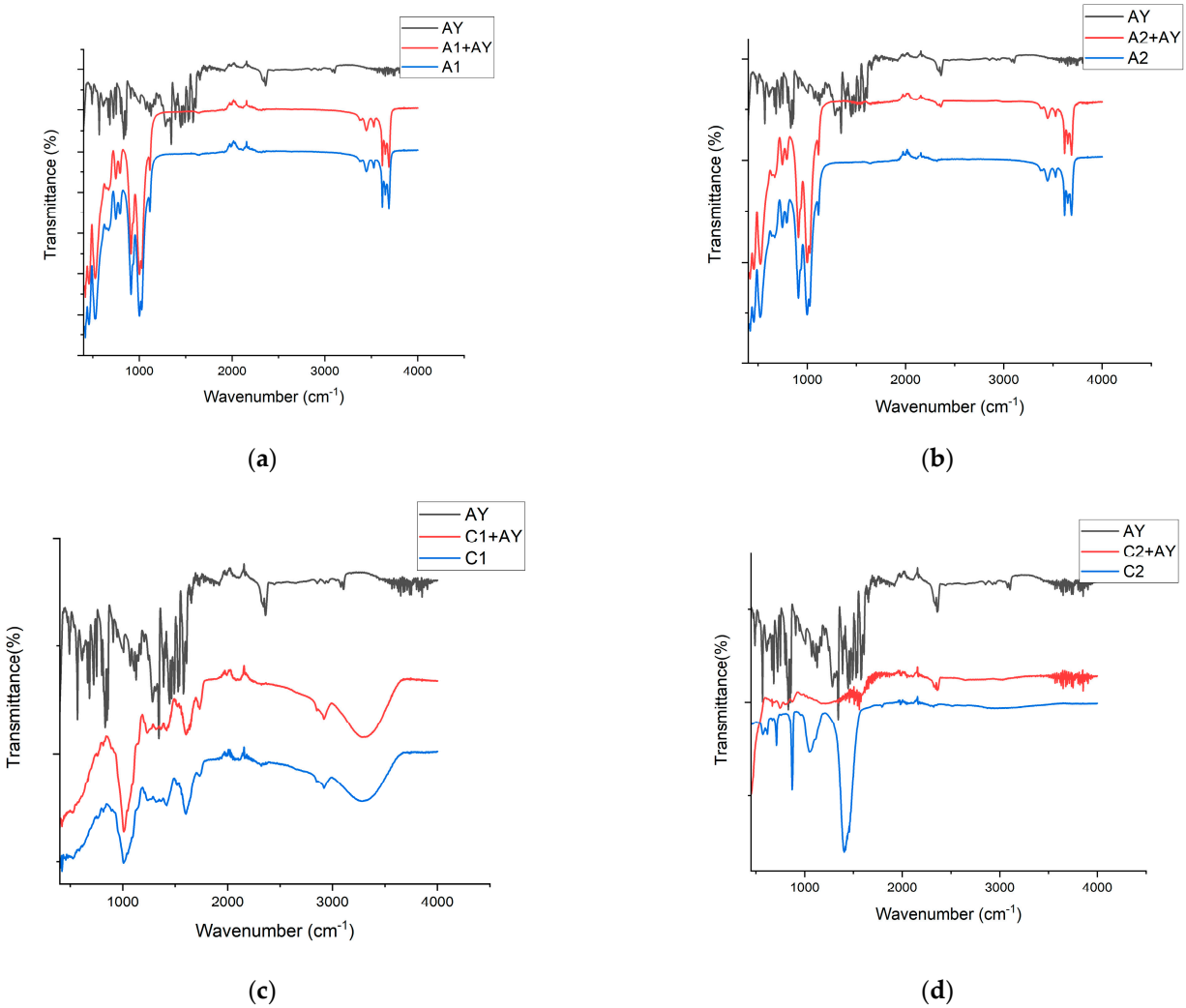

Figure 2. The FTIR spectra of AY dye and the adsorbents—before and after AY adsorption ((**a**) A1; A1+AY; (**b**) A2; A2+AY; (**c**) C1; C1+AY; (**d**) C2; C2+AY).

The FTIR spectra of natural clay adsorbents (A1 and A2) before and after AY dye adsorption were very similar (Figure 2a,b). The difference was a slight decrease in absorbance for the bands at 3694 cm^{-1} and 917 cm^{-1}, which demonstrated that Al–Al–O bonds participated in the adsorption process of AY.

The FTIR spectra of the orange-peel-based adsorbents C1 and C2—before and after AY dye loading—were very similar (Figure 2c,d). An obvious decrease in adsorption characteristic peaks at 3300 and 1022 cm^{-1} confirmed that –OH and C–O functional groups participated in the sorption process of AY dye.

3.1.3. Thermogravimetric Analysis (TGA)

The thermal stability of adsorbent materials was evaluated using thermogravimetric analysis (TGA). A thermo-differential thermal synchronization analyzer was used for the thermogravimetric analysis. The TGA-DTG curves for the adsorbents were generated from room temperature to 700 °C, and they are shown in Figure 3. The orange peel degradation profile indicates three main weight losses. The mass loss of 4.74% observed below 110 °C is attributed to the dehydration of the sample, while the steps of 55.88% loss recorded between 167 and 362 °C are due to the degradation of cellulose, hemicellulose and lignin. The thermal degradation of heat-treated orange peel shows only two main thermal events: the one below 110 °C is due to absorbed water, and the second loss between 110 and 700 °C can be assigned to the residual degradation of lignin left after the heat treatment step at 400 °C. This behavior was also observed by Flores-Rojas and authors [32]. The thermogravimetric analysis of both clay samples reveals similar behavior, with two degradation steps. An intensive mass loss of almost 3% is observed from 200 °C to 311 °C, which corresponds to the elimination of impurities by decomposition and surface moisture. The second weight loss of 11.7% is observed between 312 and 660 °C and, according to Kassa and authors [33], is caused by the dehydroxylation step.

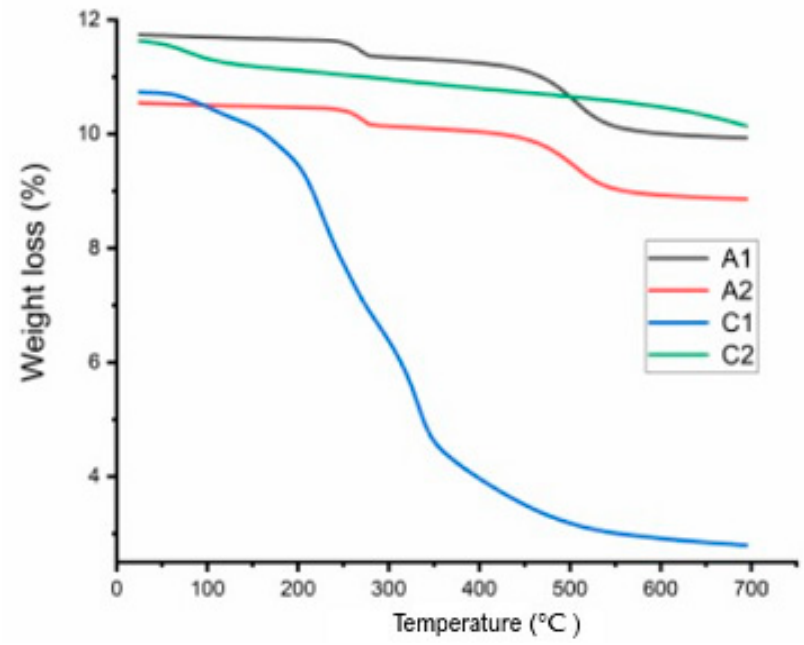

Figure 3. TGA curves of adsorbent samples prepared from natural clay (A1, A2) and adsorbent samples prepared from orange peel waste (C1, C2).

3.1.4. Surface Area Determination

The surface area of the adsorbents was determined from N_2 adsorption isotherms using Brunauer–Emmett–Teller (BET) analysis. The Barrett–Joyner–Halenda (BJH) model was employed to determine the specific pore volume and pore area by the adsorption and desorption technique.

The specific surface area, total pore volume and pore diameter (nm) are summarized in Table 1. Comparing the C1 and C2 adsorbents, it can be observed that at high temperatures, the organic matter in the orange peel decomposes, increasing the specific surface area [34]. After the heat treatment, in addition to the specific surface, the total volume of the pores also increases. According to the International Association for Pure and Applied Chemistry (IUPAC), the pores of all adsorbents belong to the category of mesopores, with pore sizes between 2 and 50 nm [35,36]. The adsorption/desorption isotherms of adsorbents A1 and C2 can be assigned to a type III isotherm with an H1 loop (A1) and a type IV isotherm with a loop of type H4, respectively, which characterizes mesoporous carbon structures

(C2 adsorbent). The desorption curve for the C2 sorbent that does not close may be due to pores that break and slit-shaped pores [37–39].

Table 1. N_2 sorption data and pore size data of adsorbents.

Sample	Specific Surface Area (m^2/g)	Total Pore Volume (cm^3/g)	Average Pore Diameter (nm)
C1	0.73	0.005	29.39
C2	170.08	0.081	2.69
A1	24.68	0.209	29.89
A2	19.35	0.145	29.39

3.2. Adsorption Performance Studies

The adsorption process can be influenced by a number of experimental factors, including temperature, contact time, *p*H, adsorbent dosage and initial dye concentration.

AY is an anionic azo dye with a *p*Ka value of 11.0 and an *ortho*-hydroxybenzoic group (Scheme 1). The color of the AY solution is yellow at *p*H 10.1, and it becomes red at *p*H 12. In aqueous solutions, the carboxyl group of AY might deprotonate. As a result, it is likely that neutral AY and its anion AY^- will coexist in the solution [5].

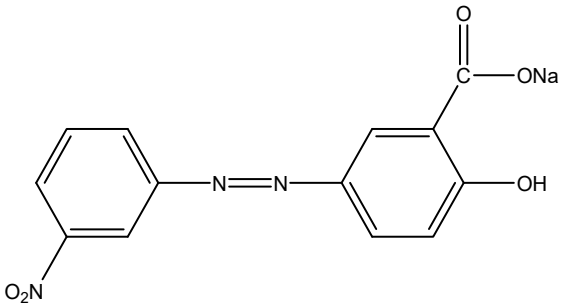

Scheme 1. Chemical structure of AY dye.

3.2.1. Effect of Initial AY Concentration

The driving force required to overcome the resistance to mass transfer of AY dye between the aqueous solution and the sorbent surface is influenced by the initial concentration of the dye solution, which is a significant factor that can alter the adsorption process [5,40].

The influence of the initial AY concentration (20–120 mg/L) on the adsorption process is presented in Figure 4a (where *p*H = 6.5, adsorbent dosage = 200 mg, volume of solution = 100 mL, contact time = 90 min, 200 rot/min). Figure 4a demonstrates that an increase in the initial concentration of AY dye caused the acceleration of the adsorption process. The highest adsorption efficiency (85.83–96.84%) and the best adsorption capacity (15.97–29.59 mg/g) occurred in a range of 30–70 mg/L for all adsorbents (Figure 4a).

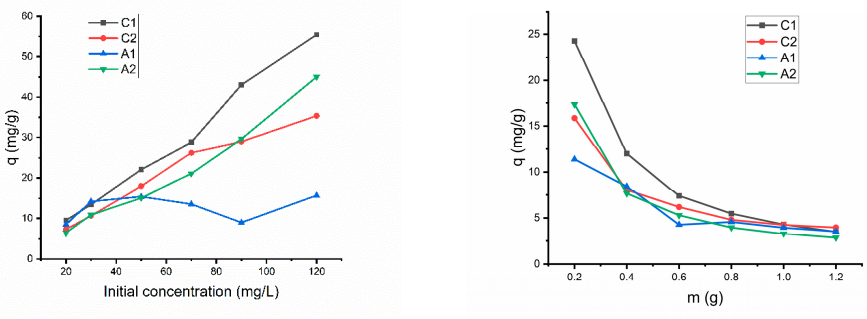

(**a**) (**b**)

Figure 4. *Cont.*

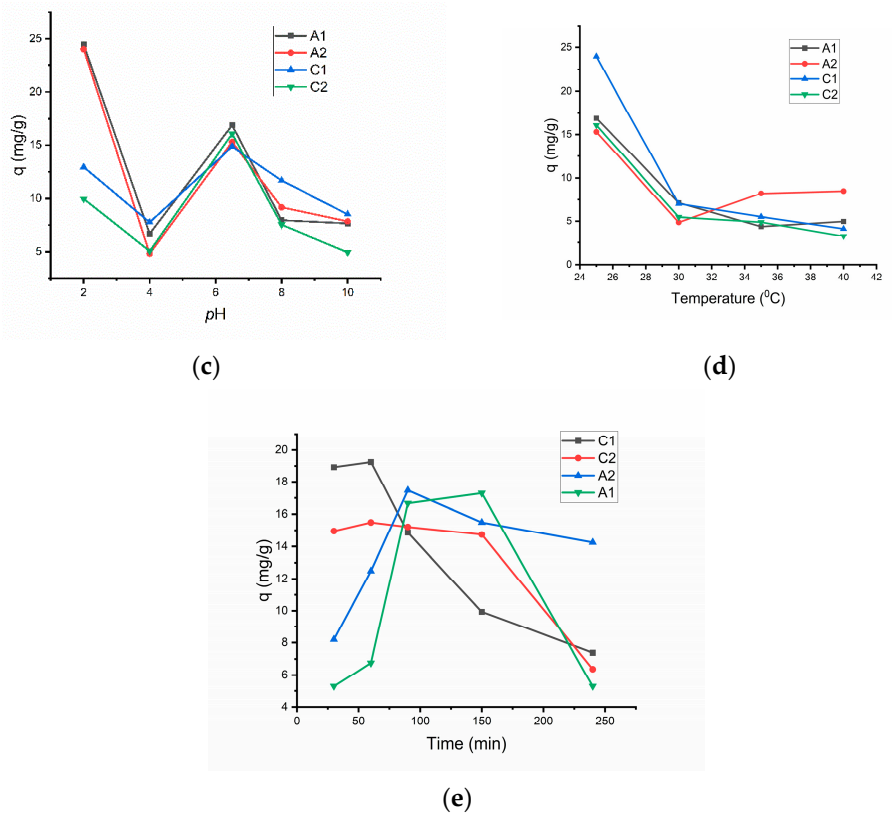

Figure 4. Effects of different parameters on the adsorption of AY dye onto the adsorbents A1, A2, C1 and C2: (**a**) initial AY concentration; (**b**) mass of sorbent; (**c**) *p*H; (**d**) temperature; (**e**) contact time.

The adsorbents prepared from orange peel waste by chemical and thermal treatments (C1 and C2) presented the best adsorption capacity compared to the other adsorbents.

3.2.2. Influence of Adsorbent Weight

The experimental results regarding the impact of the adsorbent dose on Alizarin Yellow R dye removal are presented in Figure 4b (where AY dye concentration = 50 mg/L, *p*H = 6.5, mass of adsorbent = 200 mg, volume of solution = 100 mL, time = 90 min, 200 rpm).

The capacity of adsorption for all sorbents reached the highest values with a weight of 0.2 g (17.33–24.27 mg/g), and this could be explained by the greater number of active sites available for the adsorption process (Figure 4b). In this case, an adsorbent weight of 0.2 g was selected as the optimal amount for AY dye removal.

Figure 4b shows that the capacity of adsorption at equilibrium tends to decrease when the adsorbent weight increases. The presence of more numerous active sites on the adsorbent surface in these experimental conditions could explain this variation [35,36].

3.2.3. The Influence of pH

The *p*H value plays a key role in the performance of wastewater treatment processes. Therefore, adsorption studies were performed at different *p*H values, in the range of 2–10, by adjusting *p*H with 0.1 M HCl and 0.1 M NaOH solutions. In this study, 0.2 g of each adsorbent was added to 100 mL of a 50 mg/L AY dye solution. The mixtures of adsorbent–AY dye were continuously stirred at 200 rpm and a temperature of 28 °C for a contact time of 120 min.

Figure 4c demonstrates that effective adsorption properties were obtained at *p*H = 6.5 for all types of adsorbents, and the highest adsorption capacities were registered at *p*H = 2 only for adsorbents prepared from natural clay—A1 and A2. This aspect can be explained by a decrease in H^+ on these adsorbents' surface sites and by a decrease in positive surface charge, which results in less repulsion of the adsorbing dye.

As an anionic dye, AY has a negative charge in aqueous solutions, and the adsorption process will be influenced by the solution *p*H and the charge on the surface of each adsorbent. The carboxyl group of AY could deprotonate in aqueous solutions, and as a result, the AY anion (AY^-) and the neutral species (AY) will coexist [36,41].

At *p*H < 7, interaction forces between AY and adsorbents are likely to be greater than at higher *p*H values, where these groups are negatively charged due to the protonation of the carboxyl groups of AY. At *p*H > 7, the capacity of adsorption of all adsorbents decreases, as the negatively charged adsorbent materials have fewer sites for adsorption due to increased repulsive forces. At lower *p*H, the tested sorbents prepared from orange peel waste (C1 and C2) were highly soluble in an aqueous solution. The initial *p*H of the solution affected the surface charge of each adsorbent, as well as the degree of ionization of the materials that were present in the solution.

Considering these effects, the optimal value of *p*H in the adsorption studies was 6.5 for all sorbents (A1, A2, C1 and C2).

3.2.4. Influence of Temperature

Temperature is a factor that plays an important role in the adsorption process, because it can influence the mobility of molecules in an aqueous solution and the surface properties of adsorbent materials.

The effect of temperature on the adsorption of AY dye was studied at temperatures ranging from 25 to 40 °C, and the results are shown in Figure 4d (where the experimental conditions were AY concentration = 50 mg/L; *p*H = 6.5; adsorbent weight = 200 mg; volume of solution = 100 mL, contact time = 90 min; stirring rate = 200 rpm).

The best capacities of adsorption were obtained at the temperature of 25 °C for all tested adsorbents (16.0687–24.4485 mg/g). As shown in Figure 4e, an increase in the temperature value from 25 °C to 40 °C decreases the AY capacity of adsorption. Differences in temperature affect the equilibrium capacity of the sorbents, because the diffusion rate of AY dye molecules is controlled by the temperature. The increase in diffusion could explain an increase in the adsorption amount or adsorption rate.

Some experimental conditions, for example, working at various temperatures, influence the solubility of adsorbates, and these can have a substantial impact on the adsorption process [42,43].

3.2.5. Influence of Contact Time

The effect of contact time (30–240 min) was studied for the adsorption of AY dye at an initial dye concentration of 50 mg/L and an adsorbent dose of 200 mg using biosorbents prepared from natural clay and orange peel waste—A1, A2, C1 and C2 (Figure 4e).

As shown in Figure 4e, the adsorption capacity of AY dye increased significantly during the first 60 min because there were many active sites on the adsorption surface. The best values of adsorption capacity for all adsorbents were obtained at 90 min (14.864–17.4635 mg/g). At 150 and 240 min, the external pores of the adsorbents were saturated, and the adsorption capacity decreased. Therefore, 90 min was determined to be the optimal contact time for adsorption studies.

3.3. Equilibrium Adsorption Studies

To describe the adsorption process of AY dye on adsorbents prepared from natural clay (A1, A2) and orange peel waste (C1, C2) and to analyze the behavior in a heterogeneous solid–liquid adsorption system in detail, the equilibrium adsorption results were studied using different adsorption isotherms, including the Langmuir, Freundlich and Temkin models. The most common and traditional approach is the linear fitting of these isotherm models.

3.3.1. Langmuir Model

The Langmuir isotherm model is based on the assumptions of Langmuir theory, which assumes that adsorption occurs through the formation of an adsorbate monolayer and a near-equilibrium process with active sites homogeneously distributed on the surface [3,44].

The Langmuir isotherm's linearized form is commonly obtained through Equation (3):

$$\frac{C_e}{q_e} = \frac{C_e}{q_m} + \frac{1}{q_m \cdot K_L} \quad (3)$$

where q_e represents the equilibrium adsorption capacity (mg g^{-1}); q_m is the maximum capacity of adsorption (mg g^{-1}); C_e represents the equilibrium adsorbate (AY dye) concentration (mg/L); and K_L is the Langmuir equilibrium constant (L mg^{-1}).

A plot of C_e/q_e versus C_e was employed to obtain the values of the parameters q_m and K_L (Figure 5a). The corresponding values calculated by using the Langmuir isotherm are presented in Table 2.

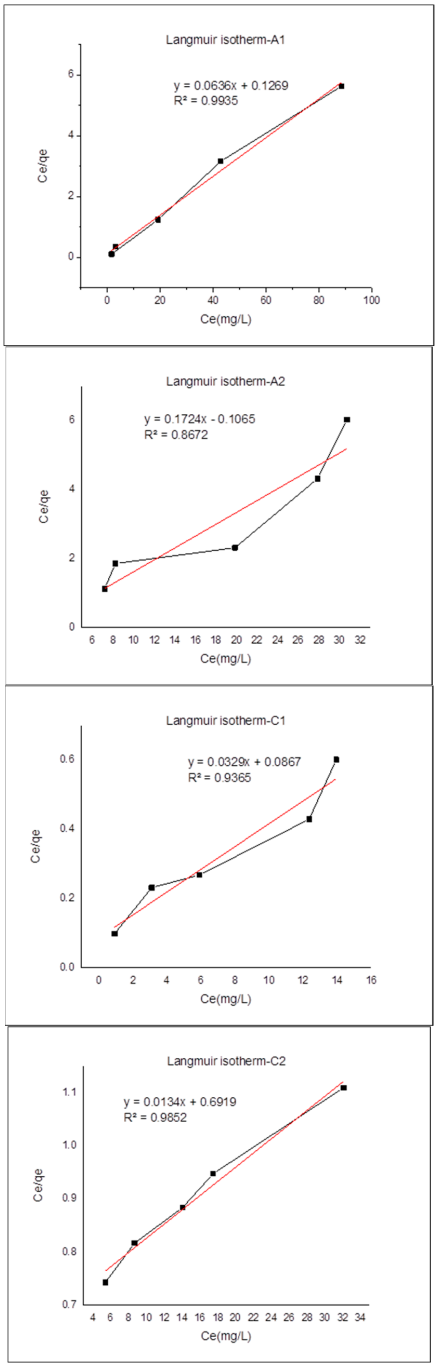

(**a**)

Figure 5. *Cont.*

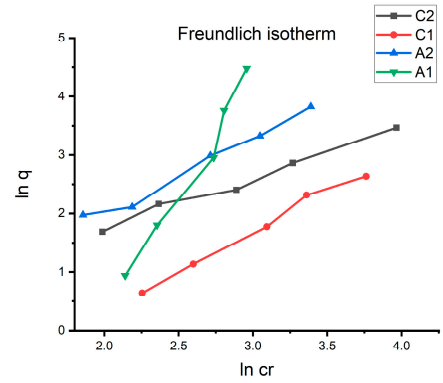

(**b**)

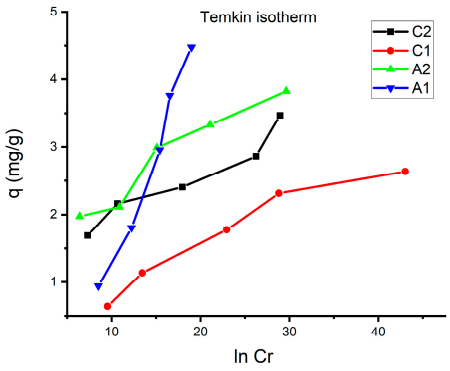

(**c**)

Figure 5. Adsorption isotherms applied to the adsorption of AY dye on A1, A2, C1 and C2 sorbents: Langmuir (**a**), Freundlich (**b**) and Temkin (**c**).

Table 2. The validity of the Langmuir model using the separation factor R_L.

The Separation Factor (R_L)	The Validity of the Adsorption Process
$R_L = 1$	Linear
$R_L > 1$	Unfavorable
$0 > R_L < 1$	Favorable; a reversible process
$R_L \rightarrow 0$	Irreversible process

The validity of the Langmuir isotherm model can be proved through a constant—a dimensionless separation factor R_L, which is calculated through Equation (4):

$$R_L = \frac{1}{1 + K_L \cdot C_i} \quad (4)$$

The value obtained for the separation factor R_L indicates whether the process of adsorption is favorable or unfavorable in the experimental conditions, and it also shows the reversibility of this process [3,45].

3.3.2. Freundlich Model

The Freundlich isotherm model assumes the possibility of a multilayer adsorption mechanism occurring on a heterogeneous surface, and it is mathematically described through the linearized form, according to Equation (5):

$$\ln\ q_e = \ln\ K_F + \frac{1}{n} \ln C_e \quad (5)$$

K_F is the capacity of adsorption (mg g^{-1}) (L $mg^{-1})^{1/n}$; n represents a dimensionless parameter proportional to the intensity of adsorption; q_e (mg g^{-1}) represents the equilibrium concentration of dye per gram of adsorbent; and C_e is the concentration of AY dye at equilibrium (mg/L).

The corresponding values calculated by using the Freundlich isotherm are presented in Table 3. K_F and n values were calculated from the plot of ln q_e vs. ln C_e (Figure 5b). The ratio $1/n$ obtained from the Freundlich isotherm model indicates a favorable adsorption process for the domain between 0 and 1; when the ratio $1/n = 1$, this demonstrates the absence of interaction between adsorbed species; if $1/n > 1$, the adsorption process is considered unfavorable [3,4,31].

Table 3. Characteristic parameters calculated from Langmuir, Freundlich and Temkin models.

Adsorbent Material	Langmuir Isotherm	Freundlich Isotherm	Temkin Isotherm
Natural clay (A1)	R^2 = 0.9935 q_m = 15.7232 mg/g K_L = 0.5012 L/mg ΔG = +1.7286 kJ/mol R_L = 0.0383 (C_i = 50 mg/L)	R^2 = 0.9736 K_F = 6.4450 mg/g n_F = 1.243	R^2 = 0.9771 K_T = 1.0063 L/g b_T = 7.1808 kJ/mol
Natural clay—chemically treated (A2)	R^2 = 0.8672 q_m = 15.8004 mg/g K_L = 0.6207 L/mg ΔG = +1.1934 kJ/mol R_L = 0.0121 (C_i = 50 mg/L)	R^2 = 0.9821 K_F = 3.5300 mg/g n_F = 2.071	R^2 = 0.9352 K_T = 1.0244 L/g b_T = 29.6155 kJ/mol
Orange peel waste—chemically treated (C1)	R^2 = 0.9365 q_m = 30.3951 mg/g K_L = 0.3794 L/mg ΔG = +2.4253 kJ/mol R_L = 0.0502 (C_i = 50 mg/L)	R^2 = 0.9894 K_F = 3.9110 mg/g n_F = 4.150	R^2 = 0.9243 K_T = 1.0050 L/g b_T = 42.1298 kJ/mol
Orange peel waste—thermally treated (C2)	R^2 = 0.9852 q_m = 74.6268 mg/g K_L = 0.0193 L/mg ΔG = +9.8790 kJ/mol R_L = 0.5102 (C_i = 50 mg/L)	R^2 = 0.9867 K_F = 2.3962 mg/g n_F = 8.33	R^2 = 0.9295 K_T = 1.0181 L/g b_T = 36.0073 kJ/mol

3.3.3. Temkin Model

The main assumption of the Temkin isotherm model is based on thermal changes during adsorption phenomena, taking into account the interactions between the adsorbent and adsorbate [3,31]. The equation of the Temkin model is the following:

$$q = \frac{RT}{b}\ln(K_T \cdot C_e) \quad (6)$$

where K_T represents the Temkin model constant (L g^{-1}); b corresponds to the Temkin constant related to the heat of sorption (J·mol^{-1}); R represents the universal gas constant (8.314 J mol^{-1} K^{-1}); and T is the absolute temperature (K) [45–47]. The graph of q_e versus ln C_e (Figure 5c) was used to calculate the specific parameters of the Temkin isotherm, and these are listed in Table 3.

The parameter n_F obtained from the Freundlich model indicates the intensity of the adsorption process. If the value of n_F is either lower than 1 or higher than 1, it indicates that the adsorption process is related to either a chemical or favorable physical process.

Table 3 shows that all n_F values are greater than 1, which indicates that the adsorption process for AY removal is favorable [3,4].

The results obtained from the experimental adsorption studies were best fitted to the Freundlich isotherm (regression coefficient (R^2) = 0.9821 for A2, R^2 = 0.9894 for C1 and

R^2 = 0.9867 for C2). These observations indicate a multilayer mechanism of adsorption on the surfaces of the adsorbents A2, C1 and C2 [3,4,47].

The Langmuir isotherm indicated the best result for the natural clay adsorbent A1 (the value R^2 = 0.9935 was obtained). This result indicates the monolayer adsorption of the surface of adsorbent A1 [3–9,47].

The R_L values (Table 3, Figure 6) obtained with all types of adsorbents (A1, A2, C1, C2) for AY dye was <1, which demonstrates the efficient adsorption of AY on the tested adsorbents [26].

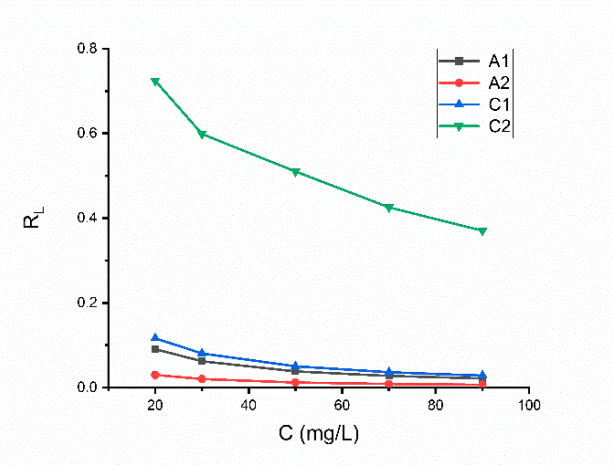

Figure 6. Separation factor R_L calculated for AY adsorption on tested adsorbents (A1; A2; C1; C2).

The adsorption-specific parameter b_T determined from the Temkin model indicated that electrostatic interactions participate in the adsorption process of AY dye on the natural clay adsorbent A1 [26]. FTIR, BET and SEM analyses of the C1 and C2 adsorbents, together with their isotherm models, showed that there were two sorption mechanisms for AY—due to functional groups and due to physical adsorption in the mesopores on the surface [3,4,9,26].

3.4. Thermodynamic Analysis

A thermodynamic study is crucial for determining the type of adsorption process and its mechanism. The thermodynamic parameters of AY adsorption on various adsorbents were determined at different temperatures, 25 °C, 30 °C, 35 °C and 40 °C. The diffusion rate of dye molecules is controlled by the temperature, and variation in the temperature influences the equilibrium capacity of sorbents. The following specific thermodynamic parameters were calculated: the change in Gibbs free energy (ΔG), enthalpy change (ΔH) and entropy change (ΔS). The results of the thermodynamic studies were interpreted, and we assessed the spontaneous nature and the thermodynamic feasibility of the adsorption processes. The following equations were used [45–50]:

$$\Delta G = -RT \ln K_L \quad (7)$$

In Equation (7), R represents the universal gas constant (8.314×10^{-3} kJ/mol K); T is the temperature (K); and K_L is the Langmuir constant of the adsorption process.

By plotting ln K_d against 1/T, the enthalpy change was determined, and the entropy change was calculated from the intercept (Figure S2—Supplementary Materials). The linear Van't Hoff Equation (8) was used:

$$\ln K_L = \frac{\Delta S}{R} - \frac{\Delta H}{RT} \quad (8)$$

$$\Delta G = \Delta H - T\Delta S \quad (9)$$

The thermodynamic parameters are presented in Table 4.

The results obtained for $\Delta G > 0$ suggested that the adsorption process was non-spontaneous, and it needed a smaller amount of energy for the adsorbents A1, C1 and C2. The negative values of Gibbs free energy ($\Delta G < 0$) for the A2 adsorbent showed that the sorption process was spontaneous, and it also confirmed the good feasibility of AY adsorption in this case. Values of ΔG in the range 0–20 kJ/mole indicate a physisorption mechanism, and chemisorption is the dominating mechanism if ΔG is between 80 and 400 kJ/mole [45,50].

Table 4. The results of the thermodynamic study for AY adsorption.

Adsorbent	*T* (K)	Δ*G* (kJ/mol)	Δ*S* (J/mol·K)	Δ*H* (kJ/mol)
Natural clay adsorbent A1	298	+1.709	−35.26	−8.80
	303	+1.738		
	308	+1.766		
	313	+1.795		
Natural clay adsorbent—chemically treated A2	298	−1.196	+15.28	+3.36
	303	−1.216		
	308	−1.236		
	313	−1.256		
Orange peel waste—chemically treated C1	298	+2.401	−11.37	−0.93
	303	+2.441		
	308	+2.481		
	313	+2.521		
Orange peel waste—thermally treated C2	298	+9.778	−78.51	−13.62
	303	+9.824		
	308	+9.881		
	313	+9.913		

The negative values obtained for ΔH (adsorption studies using the adsorbents A1, C1, C2) demonstrated that an exothermic process occurred in these cases. The positive values of ΔH indicated an endothermic process when the adsorbent A2 was used [48].

The negative values of ΔS for the adsorbents A1, C1 and C2 indicated that randomness decreased at the adsorbent–AY solution interface during the adsorption process. The positive value of ΔS calculated for the adsorbent A2 indicated an irreversible and more stable adsorption process. In this case, an increase in the degree of freedom for the adsorbed AY molecules occurred [45,49,50].

3.5. Adsorption Kinetics

The study of adsorption kinetics provides information about the mechanism of adsorption, such as chemical reactions, diffusion control and mass transfer, which represent the efficiency of the process. The linear regression correlation coefficient (R^2) values (Table 5) were used to select the best-fit model (Figures 7 and 8).

Table 5. Kinetic parameters for AY adsorption (experimental conditions: initial concentration 50 mg/L, adsorbent dose 200 mg, contact time 30–240 min and *p*H 6.5 for AY dye adsorption).

Kinetic Models	A1 Adsorbent	A2 Adsorbent	C1 Adsorbent	C2 Adsorbent
Pseudo-first-order				
q_e (mg g^{-1})	-	-	16.565	15.731
k_1 (min^{-1})	-	-	0.043	0.051

Table 5. *Cont.*

Kinetic Models	A1 Adsorbent	A2 Adsorbent	C1 Adsorbent	C2 Adsorbent
R^2	-	-	0.9509	0.8662
Pseudo-second-order				
q_e (mg g^{-1})	26.366	36.990	37.133	33.460
k_2 (g mg^{-1} min^{-1})	0.018	0.010	0.029	0.013
R^2	0.7472	0.9672	0.9859	0.8796

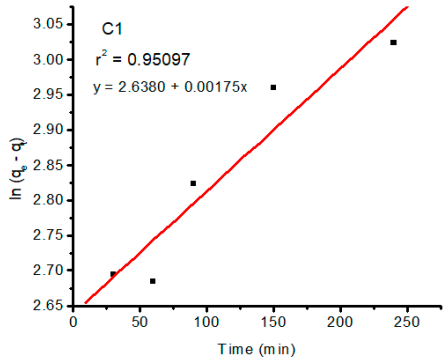

(**a**)

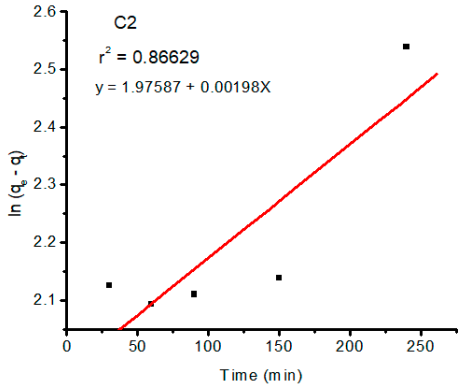

(**b**)

Figure 7. The pseudo-first rate plots for AY dye—(**a**) C1 adsorbent; (**b**) C2 adsorbent (the best fit for this model).

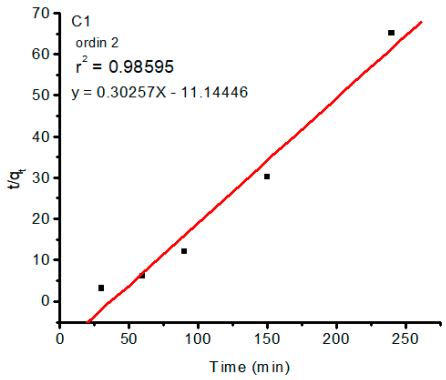

Figure 8. The pseudo-second-order plot for AY dye—C1 adsorbent (the best fit for this model).

The values of q_e and k_1 were calculated from the kinetic data through the non-linear regression of the kinetic data. The adsorption kinetics of adsorbents are usually simulated by pseudo-first- and pseudo-second-order kinetic models. The pseudo-first-order adsorption kinetic equation is the following linear form [48–54]:

$$\ln (q_e - q_t) = \ln q_e - k_1 \cdot t \quad (10)$$

where q_e represents the amount of AY adsorbed at equilibrium (mg g^{-1}), q_t is the amount of dye adsorbed at any moment (mg g^{-1}), and k_1 represents the adsorption rate constant of the pseudo-first-order kinetic equation (L min^{-1}).

The commonly used pseudo-second-order adsorption kinetic equation is the following [49–54]:

$$\frac{t}{q_t} = \frac{1}{k_2 \cdot q_e^2} + \frac{t}{q_e} \quad (11)$$

In this equation, k_2 represents the adsorption rate constant of the pseudo-second-order kinetic model [g (mg min^{-1})].

The pseudo-second-order model fit optimally for all adsorbents, with the best R^2 coefficient of 0.9859 for the C1 adsorbent. It was observed from these findings that the pseudo-second-order model, compared to the pseudo-first-order model, was fitted with higher linearity according to R^2 values (Table 5). The results were not correlated to the pseudo-first-order model for the adsorbents A1 and A2, which suggested that the rate-limiting step might not be mass transport. Based on the kinetic model obtained, a chemisorption mechanism with an electrostatic attraction was expected for the adsorption of AY on the adsorbents.

3.6. A Comparison between the Maximum Adsorption Capacity of Different Adsorbent Materials for the Removal of Alizarin Yellow R Dye

The results of the maximum adsorption capacity obtained in this study using the A1, A2, C1 and C2 adsorbents were compared to various previous studies reported in the literature (Table 6) [1,5,50–52].

Table 6. A comparison between AY dye's maximum capacity of adsorption using various adsorbent materials.

Sorbent	q_e (mg g^{-1})	Ref.
Biogenic ZnO	5.3	[4]
Fe_3O_4-PPY composite	14.93	[49]
$CuFe_2O_4$-graphene	26.3	[50]
Modified form of γ-alumina nanoparticles	98.0	[51]
A1	47.8	[52]
A2	15.72	This study
C1	15.8	This study
C2	30.39	This study
	74.62	This study

We should mention that it is difficult to make a comparison between our results and the results of these experimental studies, considering that the structures of adsorbents are different and some determining parameters are not exactly the same: the initial concentration of AY, sorbent weight, working temperature, *p*H, agitation speed and contact time.

Environmental Significance

Nanomaterial-based biosorbents have attracted increasing attention in wastewater treatment applications due to their attractive properties and strong adsorption capacities for various organic pollutants, including dyes.

This study presents various equilibrium studies on the adsorption of an AY dye pollutant by using natural materials, specifically clays and orange peels, to evaluate the

adsorption performance under different experimental conditions. Fruit waste was also carefully processed to convert it into an efficient bio-sorbent (C2), and its disposal is not devoid of environmental side effects. By this method of adsorbent preparation, we may also find a solution to the water pollution problem and a partial solution to agricultural solid waste management, for which further large-scale continuous adsorption operations are necessary.

Our research results show that natural clay and orange peel waste, which are environmentally friendly and low-cost materials, can be efficiently used to remove AY dye from aqueous solutions by adsorption. A large number of organic wastes, mainly consisting of agricultural waste, horticultural waste, forestry waste, food processing waste, sludge, etc., have recently been used for energy recovery, as value-added products or as adsorption materials for various dyes, targeted by green chemistry utilization strategies.

4. Conclusions

The present study had the objective to use efficient adsorbents derived from natural raw materials—natural clay and orange peel waste—in the removal of an anionic pollutant dye—Alizarin Yellow R (AY)—from synthetic solutions.

The morphology and structure of these sorbent materials were examined using advanced instrumental analysis methods.

The adsorption studies of AY were attained under various conditions, and the influence of the initial AY concentration, adsorbent weight, *p*H, contact time and temperature were evaluated to obtain the most favorable conditions for adsorption.

The values of the maximum adsorption capacities of these adsorbents were obtained between 15.72 and 74.62 mg/g, and they occurred in a range of 30–70 mg/L for all adsorbents.

The adsorption process was deduced through mathematical models of Freundlich, Langmuir and Temkin isotherms. The best results were obtained with the Freundlich isotherm for the adsorbents A2, C1 and C2 (the regression coefficients (R^2) = 0.9821 for A2, R^2 = 0.9894 for C1 and R^2 = 0.9867 for C2), which indicates a multilayer adsorption process on the sorbent surface. The Langmuir model produced the best result for the natural clay adsorbent A1 (the value R^2 = 0.9935 was obtained). The values of the Langmuir equilibrium parameter R_L obtained with all types of adsorbents (A1, A2, C1, C2) were <1, which could indicate the favorable adsorption process of AY anionic dye. The Temkin isotherm was also used to assess the adsorption possibilities of adsorbent materials. The binding energy values b_T calculated using the Temkin isotherm indicated that electrostatic forces participate in the adsorption of AY dye on the natural clay adsorbent (A1).

The study of the adsorption kinetics proved that they best fit the pseudo-second-order model, with the highest coefficients of determination (R^2), outperforming the pseudo-first-order model.

The chemical treatment of biomass produced more available binding sites, and the thermal treatment of orange peel waste increased pore spaces within the biomass, enhancing the capacity of adsorption. Orange peel has many oxygen-containing functional groups (-OH, O=C-O), which explains the strong polarity and good adsorption capacity. The thermal modification of orange peel biomass produced an increase in the volume of pores, which could indicate the particular properties of a good adsorption material.

Considering the results obtained from the isotherm models, the thermodynamic study and the kinetic study, it can be concluded that the main mechanism involved in the adsorption process was physisorption (for A1 and A2), while chemisorption only marginally contributed to the process. FTIR, BET and SEM analyses of the C1 and C2 adsorbents, together with their isotherm models, showed that there were two sorption mechanisms for AY—due to functional groups and due to physical adsorption in the mesopores on the surface.

The results of this research indicate that natural kaolinite clay (A1), acid-modified natural clay (A2), chemically treated orange peels (C1) and biochar obtained from thermally

treated orange peel waste (C2) have great potential in practical applications as green, low-cost materials for the adsorption of AY anionic dye from wastewater.

Supplementary Materials: The following supporting information can be downloaded at https://www.mdpi.com/article/10.3390/pr12051032/s1: Figure S1. EDS images of mapping of the adsorbent samples before AY dye adsorption—a. A1; b. A2; c. C1; d. C2. Figure S2. N2 adsorption-desorption isotherms of adsorbents and pore size distributions of adsorbents (a) A1; (b) C2. Figure S3. Van't Hoff linear plots for the adsorbents A1, A2, C1 and C2. Table S1. Application of Van't Hoff equation to adsorption equilibria for the adsorbents A1, A2, C1 and C2.

Author Contributions: A.B. and S.M.: methodology and conceptualization; A.B., S.M. and C.C.: performance of experiments; A.B., S.M., C.C. and E.-E.S.: formal analysis and data interpretation; A.B. and S.M.: writing of the article—original draft preparation; A.B. and S.M.: review and editing; A.B., S.M., C.C. and E.-E.S.: visualization. All authors have read and agreed to the published version of the manuscript.

Funding: This work was supported by the internal funding program of the Petroleum-Gas University of Ploiesti, Romania—GISC TPP-NMOP, No. 11095.

Data Availability Statement: Data are contained within the manuscript and Supplementary Materials.

Acknowledgments: The authors are thankful to the Petroleum-Gas University of Ploiesti, Romania, and to the Faculty of Petroleum Refining and Petrochemistry for providing the materials, equipment and laboratory facilities required to successfully perform this research study.

Conflicts of Interest: The authors declare no conflicts of interest.

References

1. Prashant, M.; Dipika, J.; Arti, M. Adsorption of dyes using custard apple and wood apple waste: A review. *Indian J. Chem.* **2023**, *100*, 100948.
2. Boulahbal, M.; Abderrahmane, M.; Canle, M.; Redouane-Salah, Z.; Devanesan, S.; AlSalhi, M.; Berkani, M. Removal of the industrial azo dye crystal violet using a natural clay: Characterization, kinetic modeling, and RSM optimization. *Chemosphere* **2022**, *306*, 135516. [CrossRef] [PubMed]
3. Chaari, I.; Fakhfakh, E.; Medhioub, M.; Jamoussi, F. Comparative study on adsorption of cationic and anionic dyes by smectite rich natural clays. *J. Mol. Struct.* **2019**, *1179*, 672–677. [CrossRef]
4. Mashentseva, A.A.; Aimanova, N.A.; Parmanbek, N.; Temirgaziyev, B.S.; Barsbay, M.; Zdorovets, M.V. *Serratula coronata* L. Mediated Synthesis of ZnO Nanoparticles and Their Application for the Removal of Alizarin Yellow R by Photocatalytic Degradation and Adsorption. *Nanomaterials* **2022**, *12*, 3293. [CrossRef] [PubMed]
5. Allouss, D.; Essamlali, Y.; Amadie, O.; Chakira, A.; Zahouily, M. Response surface methodology for optimization of methylene blue adsorption onto carboxymethyl cellulose-based hydrogel beads: Adsorption kinetics, isotherm, thermodynamics and reusability studies. *RSC Adv.* **2019**, *9*, 37858. [CrossRef] [PubMed]
6. El-Nemr, M.A.; El Nemr, A.; Hassaan, M.A.; Ragab, S.; Tedone, L.; De Mastro, G.; Pantaleo, A. Microporous Activated Carbon from Pisum sativum Pods Using Various Activation Methods and Tested for Adsorption of Acid Orange 7 Dye from Water. *Molecules* **2022**, *27*, 4840. [CrossRef] [PubMed]
7. Hassaan, M.A.; El Nemr, A.; El-Zahhar, A.A.; Idris, A.M.; Alghamdi, M.M.; Sahlabji, T.; Said, T.O. Degradation mechanism of Direct Red 23 dye by advanced oxidation processes: A comparative study. *Toxin Rev.* **2022**, *41*, 38–47. [CrossRef]
8. Seyed, A.H.; Manouchehr, V.; Niyaz, M.M.; Mohtada, S. Efficient dye removal from aqueous solution by high-performance electrospun nanofibrous membranes through incorporation of SiO_2 nanoparticles. *J. Clean. Prod.* **2018**, *183*, 1197–1206. [CrossRef]
9. Ari, R.; Naoyuki, K.; Takeo, U. Adsorption characteristics of clay adsorbents—Sepiolite, kaolin and synthetic talc—For removal of Reactive Yellow 138:1. *Water Environ. J.* **2015**, *29*, 375–382. [CrossRef]
10. Mafra, M.R.; Igarashi-Mafra, L.; Zuim, D.R.; Vasques, E.C.; Ferreira, M.A. Adsorption of remazol brilliant blue on an orange peel adsorbent. *Braz. J. Chem. Eng.* **2013**, *30*, 657–665. [CrossRef]
11. Ge, Q.; Li, P.; Liu, M.; Xiao, G.; Xiao, Z.; Mao, J.; Gai, X. Removal of methylene blue by porous biochar obtained by KOH activation from bamboo biochar. *Bioresour. Bioprocess.* **2023**, *10*, 51. [CrossRef] [PubMed]
12. Verma, L.; Siddique, M.A.; Singh, J.; Bharagava, R.N. As(III) and As(V) removal by using iron impregnated biosorbents derived from waste biomass of Citrus limmeta (peel and pulp) from the aqueous solution and ground water. *J. Environ. Manag.* **2019**, *250*, 109452. [CrossRef] [PubMed]
13. Anastopoulos, I.; Kyzas, G.Z. Are the thermodynamic parameters correctly estimated in liquid-phase adsorption phenomena. *J. Mol. Liq.* **2016**, *218*, 174–185. [CrossRef]
14. Pirillo, S.; Ferreira, M.L.; Rueda, E.H. The effect of *p*H in the adsorption of Alizarin and Eriochrome Blue Black R onto iron oxides. *J. Hazard. Mater.* **2009**, *168*, 168–178. [CrossRef] [PubMed]

15. Lalliansanga; Tiwari, D.; Tiwari, A.; Shukla, A.; Shim, M.J.; Lee, S.M. Facile synthesis and characterization of Ag(NP)/TiO_2 nanocomposite: Photocatalytic efficiency of catalyst for oxidative removal of Alizarin Yellow. *Catal. Today* **2022**, *388–389*, 125–133. [CrossRef]
16. Bilal, M.; Ihsanullah, I.; Shah, M.U.H.; Reddy, A.V.B.; Aminabhavi, T.M. Recent advances in the removal of dyes from wastewater using low-cost adsorbents. *J. Environ. Manag.* **2022**, *321*, 115981. [CrossRef] [PubMed]
17. Shakya, A.; Nunez-Delgado, A.; Agarwal, T. Biochar synthesis from sweet lime peel for hexavalent chromium remediation from aqueous solution. *J. Environ. Manag.* **2019**, *251*, 109570. [CrossRef] [PubMed]
18. Vassileva, P.; Tumbalev, V.; Kichukova, D.; Voykova, D.; Kovacheva, D.; Spassova, I. Study on the Dye Removal from Aqueous Solutions by Graphene-Based Adsorbents. *Materials* **2023**, *16*, 5754. [CrossRef] [PubMed]
19. Feng, N.; Guo, X.; Liang, S. Adsorption study of copper (II) by chemically modified orange peel. *J. Hazard. Mater.* **2009**, *164*, 1286–1292. [CrossRef]
20. Dey, S.; Basha, S.R.; Babu, G.V.; Nagendra, T. Characteristic and biosorption capacities of orange peels biosorbents for removal of ammonia and nitrate from contaminated water. *Clean. Mater.* **2021**, *1*, 100001. [CrossRef]
21. Mahrous, S.; Abdel-Galil, E.A.; Mansy, M.S.; Mansy, M.S. Investigation of modifed orange peel in the removal of Cd^{2+}, Co^{2+} and Zn^{2+} from wastewater. *J. Radioanal. Nucl. Chem.* **2022**, *331*, 985–997. [CrossRef]
22. Abid, M.; Niazi, N.K.; Bibi, I.; Farooqi, A.; Ok, Y.S.; Kunhikrishnan, A.; Ali, F.; Ali, S.; Igalavithana, A.D.; Ashad, M. Arsenic(V) biosorption by charred orange peel in aqueous environments. *Int. J. Phytoremediat.* **2016**, *18*, 442–449. [CrossRef]
23. Kuman, K.; Patavardhan, S.S.; Lobo, S.; Gonsalves, R. Equilibrium study of dried orange peel for its efficiency in removal of cupric ions from water. *Int. J. Phytoremediat.* **2018**, *20*, 593–598. [CrossRef] [PubMed]
24. Ramutshatsha-Makhwedzha, D.; Mavhungu, A.; Moropeng, M.L.; Mbaya, R. Activated carbon derived from waste orange and lemon peels for the adsorption of methyl orange and methylene blue dyes from wastewater. *Heliyon* **2022**, *8*, e09930. [CrossRef] [PubMed]
25. Kenes, K.; Yerdos, O.; Zulkhair, M.; Yerlan, D. Study on the effectiveness of thermally treated rice husks for petroleum adsorption. *J. Non-Cryst. Solids* **2012**, *358*, 2964–2969. [CrossRef]
26. Kumar, P.S.; Fernando, P.S.A.; Ahmed, R.T.; Srinath, R.; Priyadharshini, M.; Vignesh, M.; Thanjiappan, A. Effect of temperature on the adsorption of methylene blue dye onto sulfuric acid–treated orange peel. *Chem. Eng. Commun.* **2014**, *201*, 1526–1547. [CrossRef]
27. Romero-Cano, L.A.; García-Rosero, H.; Gonzalez-Gutierrez, L.V.; Baldenegro-Pérez, L.A.; Carrasco-Marín, F. Functionalized adsorbents prepared from fruit peels: Equilibrium, kinetic and thermodynamic studies for copper adsorption in aqueous solution. *J. Clean. Prod.* **2017**, *162*, 195–204. [CrossRef]
28. Awasthi, A.; Jadhao, P.; Kumari, K. Clay nano-adsorbent: Structures, applications and mechanism for water treatment. *SN Appl. Sci.* **2019**, *1*, 1076. [CrossRef]
29. Chaari, I.; Fakhfakh, J.; Moussi, B. Interactions of the dye, C.I. direct orange 34 with natural clay. *J. Alloys Compd.* **2015**, *647*, 720–727. [CrossRef]
30. Phuong, N.T.X.; Hong, N.T.T.; Kim Le, P.T.; Do, T.C. Chemically Treated Orange Peels as a Bio-adsorbent for Various Dyes. *Chem. Eng. Trans.* **2021**, *89*, 79–84. [CrossRef]
31. Deshmukh, S.; Topare, N.S.; Raut-Jadhav, S.; Thorat, P.V.; Bokil, S.A.; Khan, A. Orange peel activated carbon produced from waste orange peels for adsorption of methyl red. *Aqua Water Infrastruct. Ecosyst. Soc.* **2022**, *71*, 1351–1363. [CrossRef]
32. Flores-Rojas, A.I.; Díaz-Flores, P.E.; Medellín-Castillo, N.A.; Ovando-Medina, V.M.; Rodríguez-Ortiz, J.C. Biomaterials based on chitosan/orange peel as a controlled release matrix for KNO_3: Synthesis, characterization and their performance evaluation. *Iran. Polym. J.* **2020**, *29*, 1007–1017. [CrossRef]
33. Kassa, A.E.; Shibeshi, N.T.; Tizazu, B.Z. Kinetic analysis of dehydroxylation of Ethiopian kaolinite during calcination. *J. Therm. Anal. Calorim.* **2022**, *147*, 12837–12853. [CrossRef]
34. Zhang, W.; Wang, Y.; Fan, L.; Liu, X.; Cao, W.; Ai, H.; Wang, Z.; Liu, X.; Jia, H. Sorbent Properties of Orange Peel-Based Biochar for Different Pollutants in Water. *Processes* **2022**, *10*, 856. [CrossRef]
35. Abdelwahab, O.; Amin, N.K. Adsorption of phenol from aqueous solutions by Luffa cylindrica fibers: Kinetics, isotherm and thermodynamic studies. *Egypt. J. Aquat. Res.* **2013**, *39*, 215–223. [CrossRef]
36. Jiao, X.; Yu, H.; Kong, Q.; Luo, Y.; Chen, Q.; Qu, J. Theoretical mechanistic studies on the degradation of alizarin yellow R initiated by hydroxyl radical. *J. Phys. Org. Chem.* **2014**, *27*, 519–526. [CrossRef]
37. Hu, Z.; Srinivasan, M.P.; Ni, Y. Novel activation process for preparing highlymicroporous and mesoporous activated carbons. *Carbon* **2001**, *39*, 877–886. [CrossRef]
38. Fernandez, M.E.; Nunell, G.V.; Bonelli, P.R.; Cukierman, A.E. Activated carbon developed from orange peels: Batch and dynamiccompetitive adsorption of basic dyes. *Ind. Crops Prod.* **2014**, *62*, 437–445. [CrossRef]
39. Thommes, M.; Kaneko, K.; Neimark, A.V.; Olivier, J.P.; Rodriguez-Reinoso, F.; Rouquerol, J.; Sing, K.S.W. Physisorption of gases, with special reference to the evaluation of surface area and pore size distribution (IUPAC Technical Report). *Pure Appl. Chem.* **2015**, *87*, 1051–1069. [CrossRef]
40. Al-Ma'abreh, A.M.; Abuassaf, R.A.; Hmedat, D.A.; Alkhabbas, M.; Edris, G.; Hussein-Al-Ali, S.H.; Alawaideh, S. Adsorption Characteristics of Hair Dyes Removal from Aqueous Solution onto Oak Cupules Powder Coated with ZnO. *Int. J. Mol. Sci.* **2022**, *23*, 11959. [CrossRef]

41. Wu, K.; Yu, J.; Jiang, X. Multi-walled carbon nanotubes modified by polyaniline for the removal of Alizarin yellow R from aqueous solutions. *Adsorpt. Sci. Technol.* **2018**, *36*, 198–214. [CrossRef]
42. Fathy, R.; Ragab, E.; Ali, K.A. New polymeric matrix of polylactic acid/sodium alginate/carbon nanoparticles (PLA/SA/CNP) for efcient removal of methylene blue. *Chem. Pap.* **2023**, *77*, 6203–6216. [CrossRef]
43. Ali, N.S.; Jabbar, N.M.; Alardhi, S.M.; Majdi, H.S.; Albayati, T.M. Adsorption of methyl violet dye onto a prepared bio-adsorbent from date seeds: Isotherm, kinetics, and thermodynamic studies. *Heliyon* **2022**, *8*, e10276. [CrossRef] [PubMed]
44. Lim, C.L.; Bay, H.H.; Neoh, C.H.; Aris, A.; Majid, Z.A.; Ibrahim, Z. Application of zeolite-activated carbon macrocomposite for the adsorption of Acid Orange 7: Isotherm, kinetic and thermodynamic studies. *Environ. Sci. Pollut. Res.* **2013**, *20*, 7243–7255. [CrossRef]
45. Majd, M.M.; Kordzadeh-Kermani, V.; Ghalandari, V.; Askaric, A.; Sillanpää, M. Adsorption isotherm models: A comprehensive and systematic review (2010–2020). *Sci. Total Environ. 2022 812*, 151334.
46. Ayawei, N.; Ebelegi, A.N.; Wankasi, D. Modeling and Interpretation of Adsorption Isotherms. *J. Chem.* **2017**, *2017*, 3039817. [CrossRef]
47. Borhade, A.V.; Kale, A.S. Calcined eggshell as a cost effective material for removal of dyes from aqueous solution. *Appl. Water Sci.* **2017**, *7*, 4255–4268. [CrossRef]
48. Jain, S.; Jayaram, R.V. Removal of basic dyes from aqueous solution by low-cost adsorbent: Wood apple shell (*Feronia acidissima*). *Desalination* **2010**, *250*, 921–927. [CrossRef]
49. Gholivand, M.B.; Yamini, Y.; Dayeni, M.; Seidi, S.; Tahmasebi, E. Adsorptive removal of Alizarin red-S and Alizarin yellow GG from aqueous solutions using polypyrrole-coated magnetic nanoparticles. *J. Environ. Chem. Eng.* **2015**, *3*, 529–540. [CrossRef]
50. Salman, M.; Athar, M.; Shafique, U.; Din, M.I.; Rehman, R.; Akram, A.; Ali, S.Z. Adsorption modeling of Alizarin Yellow on untreated and treated charcoal. *Turk. J. Eng. Environ. Sci.* **2011**, *35*, 209–216. [CrossRef]
51. Hashemian, S.; Rahimi, M.; Kerdegari, A.A. $CuFe_2O_4$@graphene nanocomposite as a sorbent for removal of Alizarine yellow azo dye from aqueous solutions. *Desalin. Water Treat.* **2016**, *57*, 14696–14707. [CrossRef]
52. Al-Rubayee, W.T.; Abdul-Rasheed, O.F.; Ali, N.M. Preparation of a Modified Nanoalumina Sorbent for the Removal of Alizarin Yellow R and Methylene Blue Dyes from Aqueous Solutions. *J. Chem.* **2016**, *2016*, 4683859. [CrossRef]
53. Ho, Y.S.; McKay, G. Kinetic models for the sorption of dye from aqueous solution by wood. *Process Saf. Environ. Prot.* **1998**, *76*, 183–191. [CrossRef]
54. Ho, Y.S.; McKay, G. Batch lead (II) removal from aqueous solution by peat: Equilibrium and kinetics. *Trans. IchemE* **1999**, *77*, 165–173. [CrossRef]